Korean J. Chem. Eng., 17(6), 684-690 (2000)

Hydrodynamic Transition from Fixed to Fully Fluidized Beds for Three-Phase Inverse Fluidization

Dong-Hyun Lee*, Norman Epstein and John R. Grace

Department of Chemical and Biological Engineering, University of British Columbia,
2216 Main Mall, Vancouver, B.C., Canada V6T 1Z4
(*Received 7 June 2000 • accepted 18 August 2000*)

Abstract–Hydrodynamic transition experiments, involving both visual observations and pressure measurements, were performed using a 127-mm diameter Plexiglas column for three-phase inverse fluidized beds of 5.8-mm polyethylene spheres. Observations of interest not hitherto reported include: (1) A marked hysteresis effect (even when starting from a loose-packed condition) between inverse fluidization and defluidization which disappears when a wetting agent is added to the downflowing water. (2) An initially abrupt decrease of the minimum fluidization voidage, ε_{mf}, followed by a gradual rise of ε_{mf} with increasing superficial gas velocity, U_g. (3) Lower values of ε_{mf} for three-phase systems than for the corresponding two-phase (liquid-solid) fluidized beds because local agitation by the gas bubbles causes bed compaction near the minimum liquid fluidization velocity, U_{lmf}. (4) U_{lmf} vs. U_g curves which, though they always show U_{lmf} decreasing as U_g increases, sometimes display concave-downward, sometimes concave-upward and sometimes S-shaped behavior.

Key words: Inverse Fluidization, Three-Phase Fluidization, Minimum Fluidization, Hysterisis

INTRODUCTION

For three-phase inverse fluidized beds, gas flows upward and liquid downward. Typical applications are gas-liquid reactions in which a catalyst is required to enhance the conversion in chemical and biochemical industrial processes such as waste-water treatment [Shiomodiara et al., 1981; Kaul and Gadaraki, 1990; Gonzalez et al., 1992; Karamanev and Nikolov, 1996; Ramsay et al., 1996; Wright and Raper, 1996], hydrometallugy for the microbiological leaching of metals [Nikolov and Karamanev, 1987] and bioremediation of pentachlophenol-contaminated soil [Karamanev et al., 1997]. However, the gas-liquid-solid fluidized bed reactor may be the most difficult of all reacting systems to commercialized due to their extremely complicated flow behavior [Tarmy and Coulaloglou, 1992].

Few studies have been published on the hydrodynamics of three-phase inverse fluidized beds. Fan and coworkers [Chern et al., 1981, 1983, 1984; Fan et al., 1982a, b] investigated the hydrodynamic behavior of three-phase inverse semi-fluidized beds in which a liquid is the continuous phase, and presented a flow regime map for three-phase inverse fully fluidized beds. Kirshnaiah et al. [1993] correlated the minimum liquid velocity at the onset of fluidization in terms of the physical properties of the fluids, particle characteristics and system variables. Buffière and Moletta [1999], Fan et al. [1982a], Ibrahim et al. [1996] and Légile et al., 1988] studied and correlated the phase holdups for three-phase inverse fluidized beds. Karamanev and Nikolov [1992a, b] studied bed expansion and particle drag coefficient in liquid-solid inverse fluidization. They concluded that the drag coefficient of free-rising light particles could be described by the conventional law of free settling only when $Re_t<130$ and/or ρ_s exceeds approximately 900 kg/m^3. Briens et al. [1997] reported minimum liquid fluidization velocity as obtained from measurements of static-pressure gradients in three-phase inverse fluidized beds. U_{lmf} was found to decrease as the superficial gas velocity increased.

Zhang et al. [1995, 1999] reported a Gas Perturbed Liquid Model (GPLM) which could predict U_{lmf} for both conventional and inverse three-phase fluidized beds. Briens et al. [1999] reported that the effect of inhibitors on minimum fluidization could be predicted from their effect on gas holdup by adapting the GPLM. Bed voidage and phase holdups have also been measured in many particle systems [Fan et al., 1982a; Légile et al., 1988; Buffière and Moletta, 1999]. However, the bed voidage at the minimum fluidization has not been systematically studied in three-phase inverse fluidized beds, although much ε_{mf} data has been published in two-phase systems (i.e. liquid-solid and gas-solid fluidized beds).

The primary objective of this study is to characterize the hysteresis effect between inverse fluidization and defluidization in three-phase inverse fluidized beds, an aspect not previously reported. A secondary objective is to show and explain the bed voidage and the individual phase holdups at the minimum fluidization condition in such beds.

PRESSURE GRADIENT

1. Two-Phase (Liquid-Solid) Inverse Fixed or Fluidized Beds

With the z-coordinate taken as positive in the upward direction, i.e. in the direction opposite to that of the liquid flow, and with the hydrostatic head of liquid corrected for the frictional pressure gradient, the overall pressure variation in the vertical direction cor-

†To whom correspondence should be addressed.
*Current address: Korea Advanced Institute of Science and Technology, Taejon 305-701
E-mail: dhlee@mail.kaist.ac.kr

rected for the frictional pressure gradient is given by

$$\left(-\frac{dP}{dz}\right)_{ls} = \rho_l g + \left(-\frac{dp}{dz}\right)_{f,ls} \quad (1)$$

The frictional pressure gradient in two-phase (liquid-solid) inverse fluidized beds is given by

$$\left(-\frac{dp}{dz}\right)_{f,ls} = \varepsilon_s(\rho_s - \rho_l)g \quad (2)$$

Substituting Eq. (2) into Eq. (1) and rearranging, we obtain

$$\frac{1}{\rho_l g}\left(-\frac{dP}{dz}\right)_{ls} = 1 + \varepsilon_s\left(\frac{\rho_s}{\rho_l} - 1\right) \quad (3)$$

In the case of a fixed bed, $(-dp/dz)_{f,ls}$ can be expressed by the Ergun [1952] equation applied to the liquid-solid interaction as followes:

$$\left(-\frac{dp}{dz}\right)_{f,ls} = -\frac{150(1-\varepsilon_l)^2\mu_l U_l}{\varepsilon_l^3 \phi^2 d_p^2} - \frac{1.75(1-\varepsilon_l)\rho_l U_l^2}{\varepsilon_l^3 \phi d_p} \quad (4)$$

Substituting Eq. (4) to Eq. (1)

$$\left(-\frac{dP}{dz}\right)_{ls} = \rho_l g - \frac{150(1-\varepsilon_l)^2\mu_l U_l}{\varepsilon_l^3 \phi^2 d_p^2} - \frac{1.75(1-\varepsilon_l)\rho_l U_l^2}{\varepsilon_l^3 \phi d_p} \quad (5)$$

We transform that equation to

$$\frac{\left(-\frac{dP}{dz}\right)_{ls}}{\rho_l g} = 1 - \frac{150(1-\varepsilon_l)^2\mu_l U_l}{\phi^2 d_p^2 \varepsilon_l^3 \rho_l g} - \frac{1.75(1-\varepsilon_l)}{\varepsilon_l^3}\frac{U_l^2}{\phi d_p g} \quad (6)$$

Eqs. (3) and (6) can be applied if the bed height is measured and it is assumed that voidages, particle properties and the superficial liquid velocity are all uniform over the bed height so that the pressure gradient is also uniform over that height interval.

2. Three-Phase (Gas-Liquid-Solid) Inverse Fixed or Fluidized Beds

A force balance over a differential height dz of fluidized bed now yields

$$-\frac{dP}{dz} = (\varepsilon_g\rho_g + \varepsilon_l\rho_l + \varepsilon_s\rho_s)g \quad (7)$$

If it is assumed that solids buoyancy in a three-phase bed is provided only by the liquid [Zhang et al., 1995, 1998], then Eq. (2) applies to this situation. Substituting for $\varepsilon_s\rho_s g$ in Eq. (7) by means of Eq. (2) and simplifying, we obtain

$$\left(-\frac{dP}{dz}\right) = (\varepsilon_s + \varepsilon_l)\rho_l g + \varepsilon_g\rho_g g + \left(-\frac{dp}{dz}\right)_{f,ls} \quad (8)$$

Note that a different result would be generated if one were to assume that the buoyancy force acting on the solids is provided by the gas-liquid mixture [Lee et al., 1999].

In the case of a fixed bed, $(-dp/dz)_{f,ls}$ can again be expressed by the Ergun [1952] equation applied to the liquid-solid interaction. This requires that solids holdup=$\varepsilon_s/(\varepsilon_s+\varepsilon_l)$, liquid holdup=$\varepsilon_l/(\varepsilon_s+\varepsilon_l)$ and liquid superficial velocity=$U_l/(\varepsilon_s+\varepsilon_l)$. Substituting the Ergun equation accordingly for $(-dp/dz)_{f,ls}$ into Eq. (8), neglecting the term $\varepsilon_g\rho_g g$ and rearranging the results, we obtain

$$\frac{1}{\rho_l g}\left(-\frac{dP}{dz}\right) = 1 - \varepsilon_g - \frac{150\varepsilon_s^2\mu_l U_l}{\phi^2 d_p^2 \varepsilon_l^3 \rho_l g} - \frac{1.75\varepsilon_s}{\varepsilon_l^3}\frac{U_l^2}{\phi d_p g} \quad (9)$$

In three-phase inverse fixed or fluidized beds, application of Eq. (9) requires knowledge of the individual phase holdups at that given condition.

EXPERIMENTAL

Hydrodynamic transition experiments, involving both visual observations and frequent pressure measurements by differential pressure transducers (Omega, PX750-DI) connected to a large number of axially distributed pressure taps, were performed using a 127-mm diameter Plexiglas column containing the three-phase inverse fluidized beds. The total column height was 2.74 m, with a 1.83-m-high test section. Pressure taps on the wall of the column, 0.1-m intervals from 0.05 m below the stainless steel liquid distributor screen (4 mesh), which prevented the particles from rising to the top portion of the column, were connected to a differential pressure transducer. A schematic diagram of the experimental setup is shown in Fig. 1. The particles studied were 5.8-mm polyethylene spheres of 910, 930 and 946 kg/m^3 respectively, fluidized by water, or water plus 50 ppm of a wetting agent (MAKON-NF, Stepan Chemical Co.), and air. The mass of particles used was 3.5 kg and initial height of bed varied from 0.50 m to 0.54 m depending on the particle density. Gas and liquid flow rates were measured by rotameters, with U_g varied from 0 to 16.5 mm/s and U_l from 0 to 26.4 mm/s. The air was introduced from a perforated distributor containing 25 holes of 0.8-mm diameter. The liquid was pumped to the fluidization column maintaining a constant liquid flow. Note that the gas and liquid velocities used were maintained in a range in which bubble entrainment by the liquid would not occur in the lower dis-

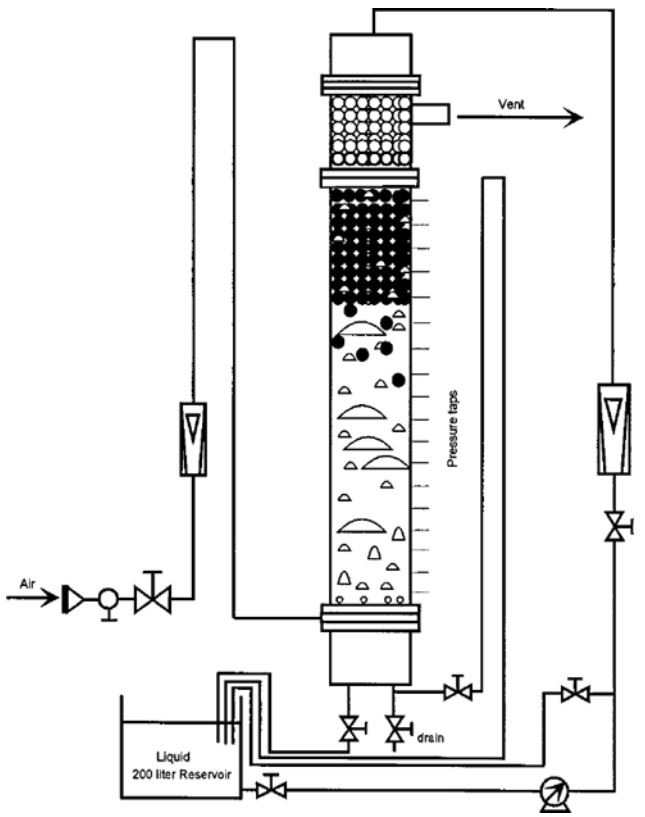

Fig. 1. Schematic diagram of experimental setup.

tributor section. Transducer signals were processed by a personal computer at a sampling frequency of 5 Hz for intervals of 180 s.

The three phase-holdups in the fluidized state were determined by solving three equations:

$$-\frac{\Delta P}{\Delta Z}=(\varepsilon_g\rho_g+\varepsilon_l\rho_l+\varepsilon_s\rho_s)g \tag{10}$$

$$\varepsilon_g+\varepsilon_l+\varepsilon_s=1.0 \tag{11}$$

$$\varepsilon_s=\frac{M_p}{\pi/4D_t^2\rho_s H_B} \tag{12}$$

The overall pressure gradients were measured also for the determination of the minimum liquid fluidization velocity of the three-phase inverse fluidized beds. For these measurements, the superficial liquid velocity was decreased step-by-step from the initially fluidized state to zero, at constant gas velocity, and then increased from zero to the fluidized state. At minimum fluidization, solids entrainment was very small, although the bed surface fluctuated. It was found that most of bed remains stationary in three-phase inverse fluidized beds when fluidization begins at the bottom of the bed. The minimum fluidization voidage, ε_{mfs} was determined from Eq. (12) by the measuring the bed height on stopping the gas flow, beyond the condition where decreasing the liquid velocity had effected a complete transition from the fluidized state to a fixed bed.

RESULTS AND DISCUSSION

1) Gas Holdup in Two-Phase (Gas-Liquid) Flow

Gas holdup was first measured in both a bubble column (U_l=0) and for countercurrent two-phase flow, with liquid flowing downward and gas upward in the absence of solid particles. Fig. 2 shows that the gas holdup increases with increasing gas velocity. There is only a small influence of liquid velocity over the range covered. In the case of the gas holdup correlation of Buffière and Moletta [1999] for bubble column (BC-R1 and BC-R2), the predicted gas holdups are higher than the present experimental results due to the smaller bubbles in the earlier study, where the gas sparger was a perforated rubber tube and a perforated membrane, respectively. The gas holdups of Briens et al. [1999] are lower than our data owing to their larger holes of the gas sparger, d_{or}=3.0 mm [Tsuchiya and Nakanishi, 1992].

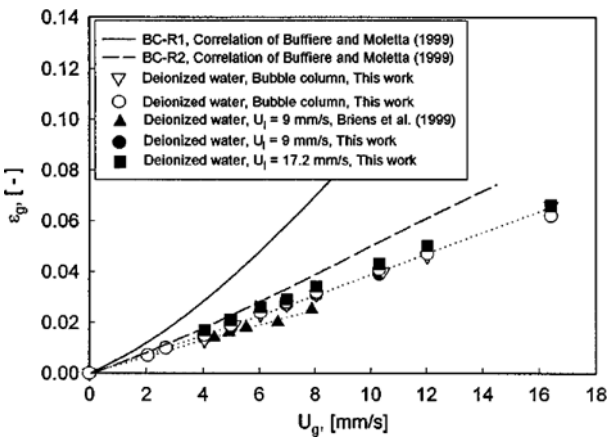

Fig. 2. Variation of gas holdup with gas superficial velocity in various bubble columns.

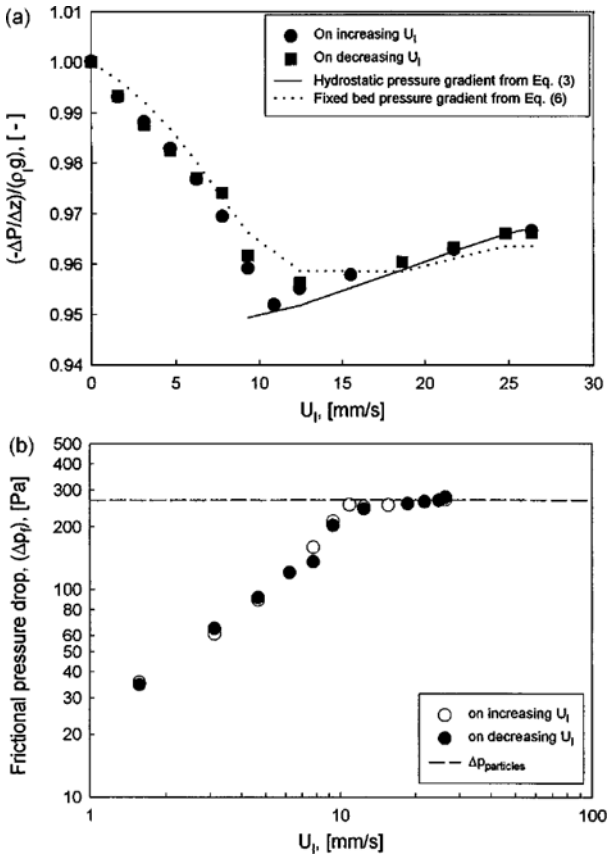

Fig. 3. Pressure gradient as function of liquid velocity for two-phase liquid-solid inverse fluidized beds. U_g=0 mm/s, d_p= 5.8 mm, ρ_s=910 kg/m^3.
(a) dimensionless pressure gradient; (b) frictional pressure drop.

2) Minimum Fluidization Velocity in Two-Phase (liquid-solid) Inverse Fluidized Beds

The minimum fluidization velocity in liquid-solid fluidized beds, U_{lmfs} is a function of the particle diameter and density, as well as of the physical properties of the liquid such as density and viscosity. The dimensionless pressure gradient for water-910 kg/m^3 polyethylene beads is shown in Fig. 3a, together with predictions for the hydrostatic pressure gradient and the fixed bed pressure gradient. The minimum liquid fluidization velocity is taken as the velocity at which the pressure gradient within the bed is a minimum. As shown in Fig. 3a, the dimensionless pressure gradient decreases initially with increasing liquid velocity, but increases gradually with increasing liquid velocity beyond U_{lmf} due to bed expansion. The frictional pressure drop, Δp_f, for the same system increases linearly with increasing liquid velocity and then reaches a constant value beyond U_{lmf}, as shown in Fig. 3b. This constant value is equal to the net buoyancy force per unit area by which the gravitational force of the particles is corrected.

3) Flow Regimes in the Three-Phase Inverse Fluidized Beds

Fig. 4 demonstrates that the frictional pressure drop profile for

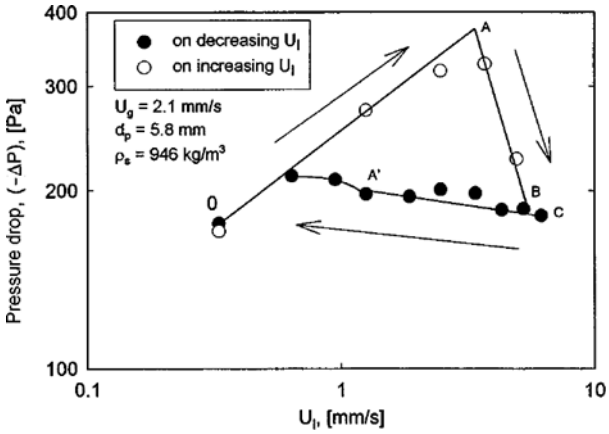

Fig. 4. Pressure drop for three-phase inverse fixed and fluidized beds of polyethylene beads.

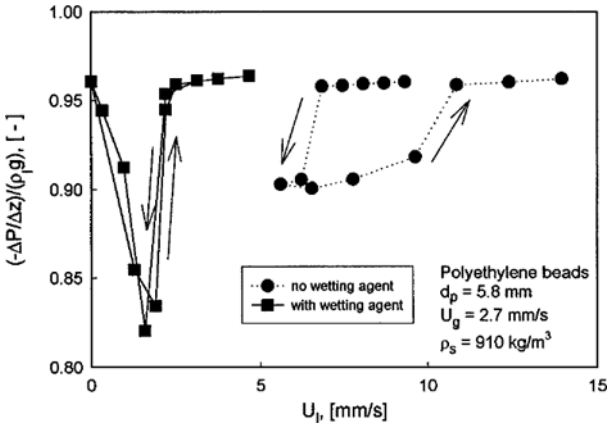

Fig. 5. Dimensionless pressure gradient profile with and without wetting agent in three-phase inverse fixed and fluidized beds for 5.8 mm polyethylene spheres of density 910 kg/m^3 at U_g=2.7 mm/s.

three-phase inverse fluidized beds differ from the profiles for two-phase inverse fluidized beds (compare Fig. 3b). Starting from a loose-packed condition, as the liquid velocity was increased, the frictional pressure drop through the bed followed a path typically described by OABC at a constant gas velocity. Three regimes are discernable in Fig. 4:

(a) Fixed-bed regime (O→A). At low U_l, the liquid simply percolates downward through the bed without disturbing the particles. The bed is maintained at a constant voidage of ε_0 and a height of H_{f0}. The magnitude of Δp_f rises steeply with increasing liquid velocity as in any fixed bed and reaches the maximum pressure drop, (Δp_{max}), at point A.

(b) Partially fluidized-bed regime (A→B). At point A and beyond, half or less of the bed is stationary, while the lower section of the bed is fluidized as mentioned by Ibrahim et al. [1996]. The frictional pressure drop, Δp_f, then decreases with increasing liquid velocity from its maximum value of (Δp_{max}) at point A to (Δp_b) at point B.

(c) Fully fluidized-bed regime (B→C). The bed reaches its initial stage of full fluidization at point B. The corresponding superficial liquid velocity is the minimum velocity of full fluidization on increasing U_l. However, when U_l is decreased, the magnitude of Δp_f follows the curve marked C→A'→O. Two flow regimes can then be identified: Segment C→A' corresponds to the fully fluidized-beds regime and segment A'→O, the fixed-beds regime. The liquid superficial velocity at A' is thus U_{lmf}.

In the fully fluidized-bed state, assuming liquid-buoyed solids, the frictional pressure drop, Δp_f, is given by:

$$\Delta p_f = \Delta p_{particles} + \Delta p_{gas} \tag{13}$$

with

$$\Delta p_{particles} = \frac{M_p g\left(\frac{\rho_l}{\rho_p} - 1\right)}{A_t} \tag{14}$$

$$\Delta p_{gas} = \frac{\rho_g \varepsilon_g V_{tot} g\left(\frac{\rho_l}{\rho_g} - 1\right)}{A_t} = \rho_g \varepsilon_g H_B g\left(\frac{\rho_l}{\rho_g} - 1\right) \tag{15}$$

From Fig. 4, on decreasing liquid velocity to U_l=1.9 mm/s, at U_g=2.1 mm/s, the bed is still in the fully fluidized state, with the bed voidage and gas holdup are 0.611 and 0.006, respectively. Substitution of these and other system values into Eqs. (14) and (15) leads to $\Delta P_{particles}$=155.0 N/m^2 and ΔP_{gas}=44.1 N/m^2. The total predicted pressure drop, Δp_f=199.1 Pa is very similar to the experimental value from Fig. 4, 195.6 Pa.

Fig. 4 exhibits substantial hysteresis in the pressure drop response to varying liquid velocity around incipient fluidization, owing apperently to the properties of interface between solid particles and liquid. Polyethylene is hydrophobic, so that air is in close contact with the particles.

Fig. 5 plots dimensionless pressure gradient profiles with and without the wetting agent. A marked hysteresis effect between inverse fluidization and defluidization occurs without a wetting agent, but disappears when the wetting agent is added. When the wetting agent was added to water, the surface tension of water decreased from 0.072 to 0.053 N/m. As a result of the addition, the gas bubbles no longer attached to the solid particles, and this eliminated the hysteresis. A similar result for a three-phase inverse turbulent bed was reported by Choi et al. [1999] who modified the surface polymer particles from hydrophobic to hydrophilic by treating the polyethylene surface with chlorosulfonic acid. They obtained a smaller critical velocity of gas bubbles than reported by Comte et al. [1997]. Also, the ranges between inverse fluidization and defluidization shifted to the left due to reducing the surface tension of liquid as the wetting agent was added to water.

4) Minimum Fluidization Velocity in Three-Phase Inverse Fluidized Beds

For conventional two-phase (liquid-solid or gas-solid) fluidization, minimum fluidization is defined as the condition at which the pressure drop across the bed equals the weight of the bed [Fan, 1989]. In the case of the two-phase (liquid-solid) inverse fluidization, minimum fluidization is defined as the condition at which the pressure drop across the bed is equal to net the buoyant force on the particles in the bed. The determination of minimum fluidization velocity in the three-phase inverse fluidized beds is more difficult because of a strong pressure drop-flow rate hysteresis. The minimum fluidization velocity at fixed U_g should be measured for

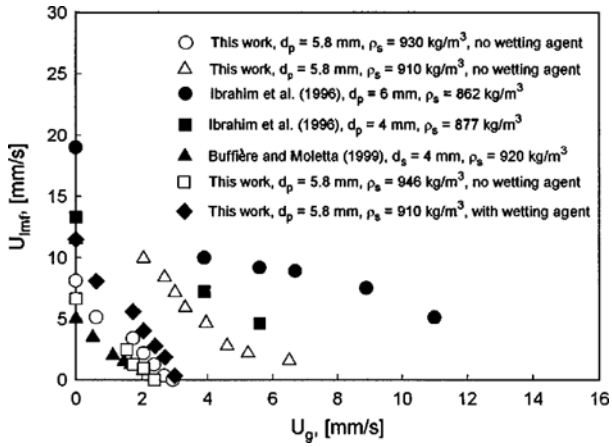

Fig. 6. Effect of gas velocity on the minimum fluidization velocity.

decreasing U_l, with minimum fluidization then defined as the condition at which the fluidized particles settle to form a fixed bed. Fig. 6 shows the variation of minimum fluidization velocity with superficial gas velocity. U_{lmf} decreased as U_g increased as in previous work [Legile et al., 1988; Ibrahim et al., 1996; Buffière and Moletta, 1999; Briens et al., 1999]. Increasing the gas velocity displaces some of the liquid, resulting in a lower liquid holdup and a larger interstitial liquid velocity. The slip velocity between liquid and particles increases and the larger drag exerted on the particles leads to early fluidization [Ibrahim et al., 1996]. However, from Fig. 6, U_{lmf} vs. U_g curves, though they always show U_{lmf} decreasing as U_g increases, sometimes display concave-downward, sometimes concave-upward and sometimes S-shape behavior. The different behavior can probably be attributed to the combined effects of liquid motion induced by the bubble rise and solid agglomerates attached to bubbles. For the 5.8-mm spheres of density 910 kg/m^3, the consistently higher downward U_{lmf} requirement with no wetting agent compared to when the wetting agent is used can be attributed to a decrease in the effective density of the particles due to bubble attachment in the absence of wetting agent, an effect which is eliminated by the wetting agent.

5) Phase Holdup and Bed Voidage of the Three-Phase Inverse Fluidized Beds

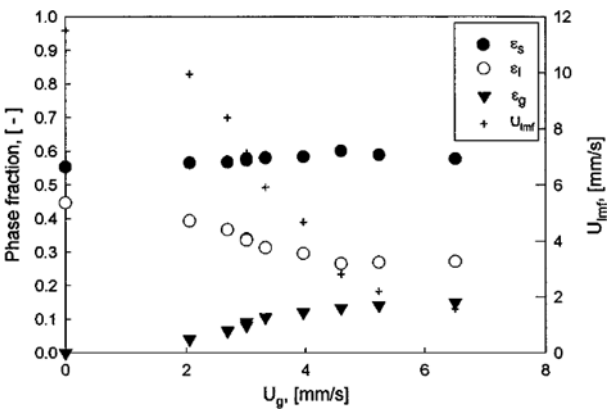

Fig. 7. Effect of gas velocity on individual phase holdups for 5.8-mm particles of density 910 kg/m^3 without wetting agent added.

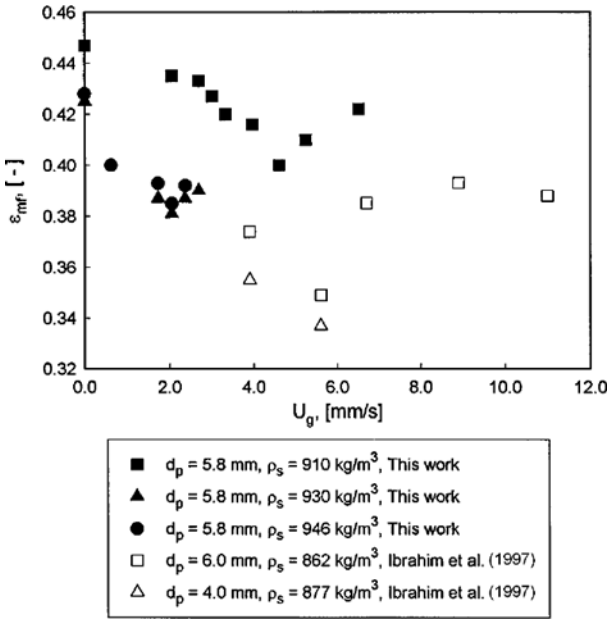

Fig. 8. Effect of gas velocity on bed voidage at minimum fluidization.

Buffière and Moletta [1999], Légile et al. [1988] and Fan et al. [1982a, b] evaluated the individual phase holdups using the estimated bed height and pressure gradient. This procedure implicitly assumes that the solid entrainment into the freeboard is negligible. Solid entrainment was in fact very small in the present study, although the bed surface fluctuated at the minimum fluidization condition, while most particles were immobile. Therefore, individual phase holdups were determined from Eqs. (10)-(12), measuring the bed height by shutting down the gas velocity after transition from the fluidized state to a fixed beds. Fig. 7 shows the individual phase holdups at the minimum fluidization condition. As expected, the gas holdup increased and the liquid holdup decreased with increasing gas velocity.

Fig. 8 shows the bed voidage at minimum fluidization, ε_{mf}, in three-phase inverse fluidized beds. In most cases there is an initial steep decrease of ε_{mf} with increasing gas velocity, followed by a gradual rise. ε_{mf} is lower than for two-phase (liquid-solid) fluidized beds, apparently because small scale agitation by the gas bubbles lead to compaction of the bed near to the minimum liquid fluidization velocity [Briens, 1997a].

CONCLUSIONS

For three-phase inverse fluidized beds with aqueous liquids, a profound hysteresis usually occurs between fluidization and defluidization, but this disappears when a wetting agent is added. The voidage at minimum fluidization, ε_{mf}, tend to fall initially to a minimum and then rise gradually with increasing superficial gas velocity. ε_{mf} is lower for three-phase systems than for the corresponding two-phase (liquid-solid) fluidized beds because local agitation by the gas bubbles causes bed compaction near the minimum liquid fluidization velocity. U_{lmf} vs. U_g curves, though they always show U_{lmf} decreasing as U_g increases, sometimes display concave-down-

ward, sometimes concave-upward and sometimes S-shaped behavior.

ACKNOWLEDGEMENT

The authors are grateful to NSERC (the Natural Sciences and Engineering Research Council of Canada) and KOSEF (the Korea Science and Engineering Foundation) for financial assistance. The authors also thank Hanwha Petrochemical Corp. and LE Chemical Co. for help in molding the polyethylene spheres.

NOMENCLATURE

A_t : cross-sectional area [m^2]
d_{or} : distributor hole diameter [m]
d_p : equivolume sphere particle diameter [mm or m]
D_t : column diameter [m]
g : acceleration of gravity [$m \cdot s^{-2}$]
H_B : bed height [m]
H_{B0} : static bed height [m]
M_p : particle inventory [kg]
ΔP : total pressure drop [Pa]
Δp_b : frictional pressure drop of the bed under fully fluidized condition [Pa]
Δp_{gas} : pressure drop of gas [Pa]
Δp_f : frictional pressure drop [Pa]
Δp_{max} : maximum frictional pressure drop trough the particle bed [Pa]
$\Delta p_{particles}$: pressure drop of particles [Pa]
$(\Delta P/\Delta z)$: total pressure gradient [Pam^{-1}]
$(-dp/dz)_{ls}$: overall pressure gradient in liquid-solid system [$Pa \cdot m^{-1}$]
$(-dp/dz)_{f,ls}$: frictional pressure gradient due to liquid-solid interaction [$Pa \cdot m^{-1}$]
U_g : superficial gas velocity [$m \cdot s^{-1}$]
U_l : superficial liquid velocity [$m \cdot s^{-1}$]
U_{lmf} : U_l at minimum fluidization [$m \cdot s^{-1}$]
V_{tot} : total volume in the bed [m^3]

Greek Letters

ε_g : gas holdup [-]
ε_l : liquid holdup [-]
ε_{mf} : voidage at minimum fluidization condition [-]
ε_0 : voidage of the fixed bed [-]
ε_s : solid holdup [-]
μ_l : liquid viscosity [$kg \cdot (m^{-1}s^{-1})$]
ρ_g : gas density [$kg \cdot m^{-3}$]
ρ_l : liquid density [$kg \cdot m^{-3}$]
ρ_s : solid density [$kg \cdot m^{-3}$]
σ : surface tension [$N \cdot m^{-1}$]
ϕ : particle sphericity [-]

REFERENCES

Briens, C. L., Ibrahim, Y. A. A., Margaritis, A. and Bergougnou, M. A., "Effect of Coalescence Inhibitors on the Performance of Three-Phase Inverse Fluidized-Bed Columns," *Chem. Eng. Sci.*, **54**, 4975 (1999).

Briens, C. L., University of Western Ontario, Personal Communication (1997a).

Briens, L. A., Briens, C. L., Margaritis, A. and Hay, J., "Minimum Liquid Fluidization Velocity in Gas-Liquid-Solid Fluidized Beds," *AIChE J.*, **43**, 1180 (1997b).

Buffiere, P. and Moletta, R., "Some Hydrodynamic Characteristics of Inverse Three Phase Fluidized-Bed Reactors," *Chem. Eng. Sci.*, **54**, 1233 (1999).

Chern, S.-H., Fan, L. S. and Muroyama, K., "Hydrodynamics of Cocurrent Gas-Liquid-Solid Semifluidization with a Liquid as the Continuous Phase," *AIChE J.*, **30**, 288 (1984).

Chern, S.-H., Muroyama, K. and Fan, L. S., "Hydrodynamics of Constrained Inverse Fluidization and Semifluidization in a Gas-Liquid-Solid System," 74th AIChE Annual Meeting, New Orleans, LA (1981).

Chern, S.-H., Muroyama, K. and Fan, L. S., "Hydrodynamics of Constrained Inverse Fluidization and Semifluidization in a Gas-Liquid-Solid System," *Chem. Eng. Sci.*, **38**, 1167 (1983).

Choi, H. S. and Shin M. S., "Hydrodynamics Study of Two Different Inverse Fluidized Reactors for the Application of Wastewater Treatment," *Korean J. Chem. Eng.*, **16**, 670 (1999).

Comte, M. P., Bastoul, D., Hebrand, G., Rouston, M. and Lazarova, V., "Hydrodynamics of a Three-Phase Fluidized Bed-The Inverse Turbulent Bed," *Chem. Eng. Sci.*, **52**, 3971 (1997).

Ergun, S., "Fluid Flow Through Packed Columns," *Chem. Eng. Prog.*, **48**, 89 (1952).

Fan, L.-S., "Gas-Liquid-Solid Fluidization Engineering," Butterworth, Stoneham, MA (1989).

Fan, L.-S., Muroyama, K. and Chern, S.-H., "Hydrodynamic Characteristics of Inverse Fluidization in Liquid-Solid and Gas-Liquid-Solid Systems," *Chem. Eng. J.*, **24**, 143 (1982a).

Fan, L.-S., Muroyama, K. and Chern, S.-H., "Some Remarks on Hydrodynamics of Inverse Gas-Liquid-Solid Fluidization," *Chem. Eng. Sci.*, **37**, 1570 (1982b).

Gonzalez, G., Ramirez, F. and Monroy, O., "Development of Biofilms in Anaerobic Reactors," *Biotechnology Letters*, **14**, 149 (1992).

Ibrahim, Y. A. A., Briens, C. B., Magaritis, A. and Bergougnou, M. A., "Hydrodynamic Charateristics of a Three-Phase Inverse Fluidized-Bed Column," *AIChE J.*, **42**, 1889 (1996).

Ibrahim, Y. A. A., University of Western Ontario, Personal Communication (1997).

Karamanev, D. G. and Nikolov, L. N., "Bed Expansion of Liquid-Solid Inverse Fluidization," *AIChE J.*, **38**, 1916 (1992b).

Karamanev, D. G. and Nikolov, L. N., "Free Rising Light Spheres Do Not Obey Newton's Law for Free Settling," *AIChE J.*, **38**, 1843 (1992a).

Karamanev, D. G., Chavarie, C. and Samson, R., "Soil Immobilization: New Concept for Biotreatment of Soil Contaminants," *Biotechn. and Bioeng.*, **57**, 471 (1997).

Kaul, S. N. and Gadaraki, S. K., "Fluidized Bed Reactor for Wastewater Treatment," *Chemical Engineering World*, **15**, 25 (1990).

Krishnaiah, K., Guru, S. and Sekar, V., "Hydrodynamic Studies on Inverse Gas-Liquid-Solid Fluidization," *Chem. Eng. J.*, **51**, 109 (1993).

Lee, D. H., Epstein, N. and Grace, J. R., "Models for Minimum Liquid Fluidization Velocity of Gas-Liquid Fluidized beds," Proceedings

of 8th APCChE Congress, 1699 (1999).
Legile, P., Menard, G., Laurent, C., Thomas, D. and Bernis, A., "Contribution to the Study of an Inverse Three-Phase Fluidized Bed Operating Countercurrently," *Intern. Chem. Enging.*, **32**, 41 (1988).
Nikolov, L. and Karamanev, D., "Experimental Study of the Inverse Fluidized Bed Biofilm Reactor," *Can. J. Chem. Eng.*, **65**, 214 (1987).
Ramsay, B. A., Wang, D., Chavarie, C., Rouleau, D. and Ramsay, J. A., "Penicillin Production in an Inverse Fluidized Bed Bioreactor," *J. of Fermentation and Bioengineering*, **72**, 495 (1991).
Shiomodiara, C., Yushina, Y., Kamata, H., Komatsu, H., Kumira, A., Mabu, O. and Tanak, Y., "Process for Biological Treatment of Waste Water in Downflow Operation," US Patent 4256573 (1981).
Tarmy, B. L. and Coulaloglou, C. A., "Alpha-Omega and Beyond Industrial View of Gas/Liquid/Solid Reactor Development," *Chem. Eng. Sci.*, **47**, 3231 (1992).
Tsuchiya, K. and Nakanishi, O., "Gas Holdup Behavior in a Tall Bubble Column with Perforated Plate Distributors," *Chem. Eng. Sci.*, **47**, 3347 (1992).
Wright, P. C. and Raper, J. A., "A Review of Some Parameters Involved in Fluidized Bed Bioreactors," *Chem. Eng. Techn.*, **19**, 50 (1996).
Zhang, J.-P., Epstein, N., Grace, J. R. and Zhu, J., "Minimum Liquid Fluidization Velocity of Gas-Liquid Fluidized beds," *Trans IChemE*, **73**, Part A, 347 (1995).
Zhang, J.-P., Epstein, N. and Grace, J. R., "Minimum Fluidization Velocities for Gas-Liquid-Solid Three-Phase Systems," *Powder Techn.*, **100**, 113 (1998).